MAGELLAN PROJECT

University of Arizona | Carnegie Institution of Washington | The Johns Hopkins University

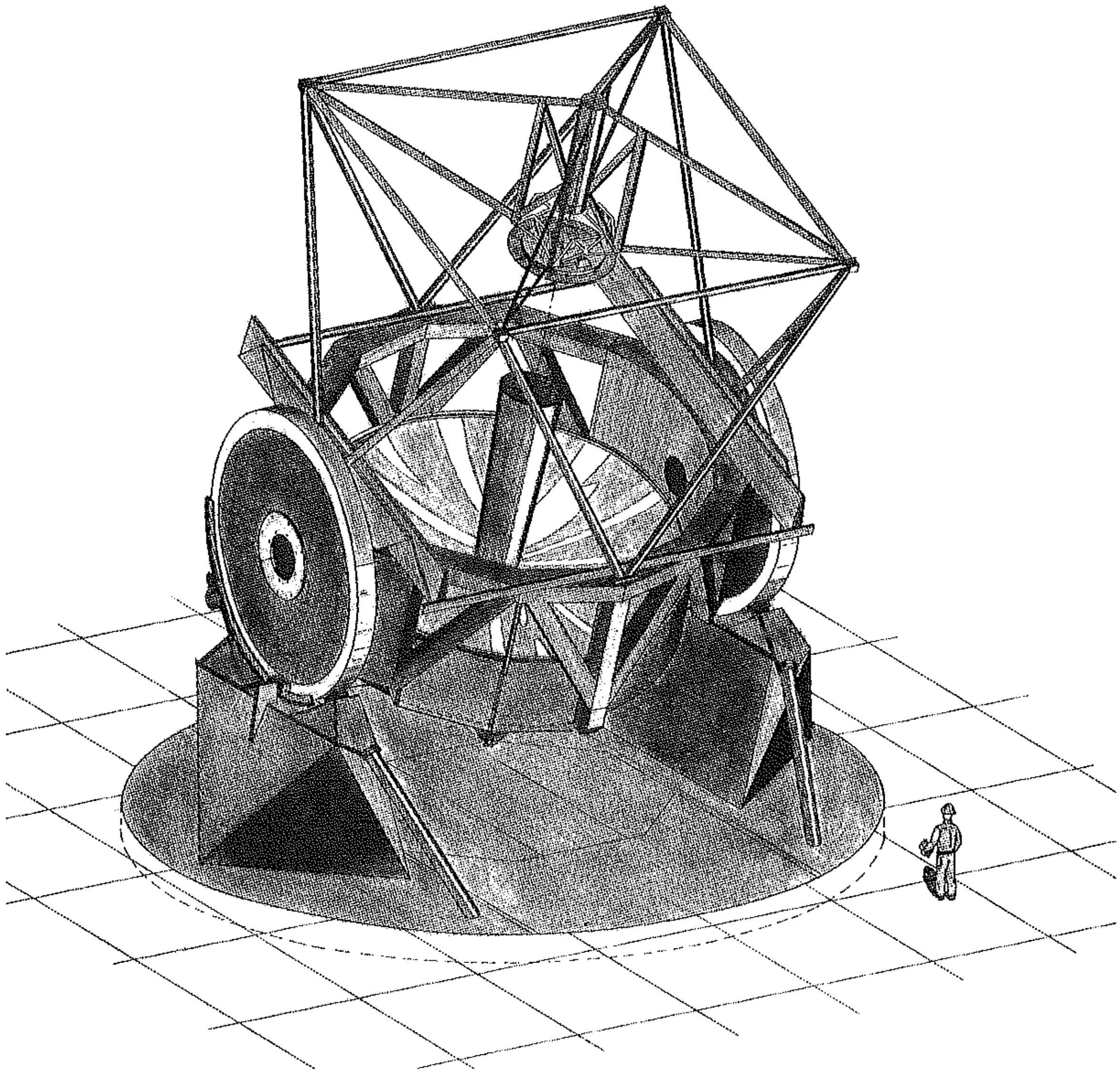

# The Effects of Drive Restraint and Pier Flexibilities


J. Alan Schier
The Observatories of the
Charnegie Institution of Washington
Pasadena, California



March 1991
No. 30

## INTRODUCTION

In this report, we examine the effects of main drive support and pier flexibilities on the performance of the main drive servos. We also take a look at some possible performance improvements through the use of inertial position measurements.

The analytical model of the telescope addresses two important structural flexibilities: one connecting the mass of the pier to ground, and the other connecting the drive box to the pier. Since we are interested here only in the first vibrational mode of the pier, it is modeled as one concentrated mass. This is also true of the drive box, although the rotational inertia of the drive line has been explicitly included in addition to the mass of the assembly. The telescope itself is treated as a rigid body; the effects of its flexibilities have been addressed in Magellan Report Nos. 28 and 29.

We assume that the telescope is driven by a single stage system such as the friction drive described in Magellan Report No. 18. The results can be extended to a multistage drive if the additional inertias are properly bookkept. The major portion of the analysis further assumes that axis position encoding is done relative to the pier. We briefly investigate the advantages of using an inertial reference for position encoding to lessen the ill effects of the flexibilities.

## SUMMARY OF RESULTS

The main results are the following two:

> 1). The pier flexibility enters the dynamics in a way that degrades the system disturbance rejection capability but does not necessarily limit the servo crossover frequency.
>
> 2). The drive box support compliance results in a vibrational mode which can limit the servo crossover frequency.

These results do not account for other possibly more critical modes that may exist in the structure. Several of these additional modes are addressed in Magellan Report Nos. 28 and 29.

A further result indicates that using an inertial reference--as opposed to referencing positions to the pier--would make the pier and drive flexibilities less important and would improve the overall system performance.

DESCRIPTION OF THE MODEL

The model used in this analysis is shown in Figure 1. It is a simplified representation of the azimuth axis of a large telescope, with four rigid bodies corresponding to the telescope rotational inertia, the drive line rotational inertia, the drive box mass, and the pier mass. The drive box is connected to the pier through a compliance representing the springiness of the drive box tangential restraint. The pier is connected to ground through a compliance that, in combination with the pier's mass, generates the first pier mode.

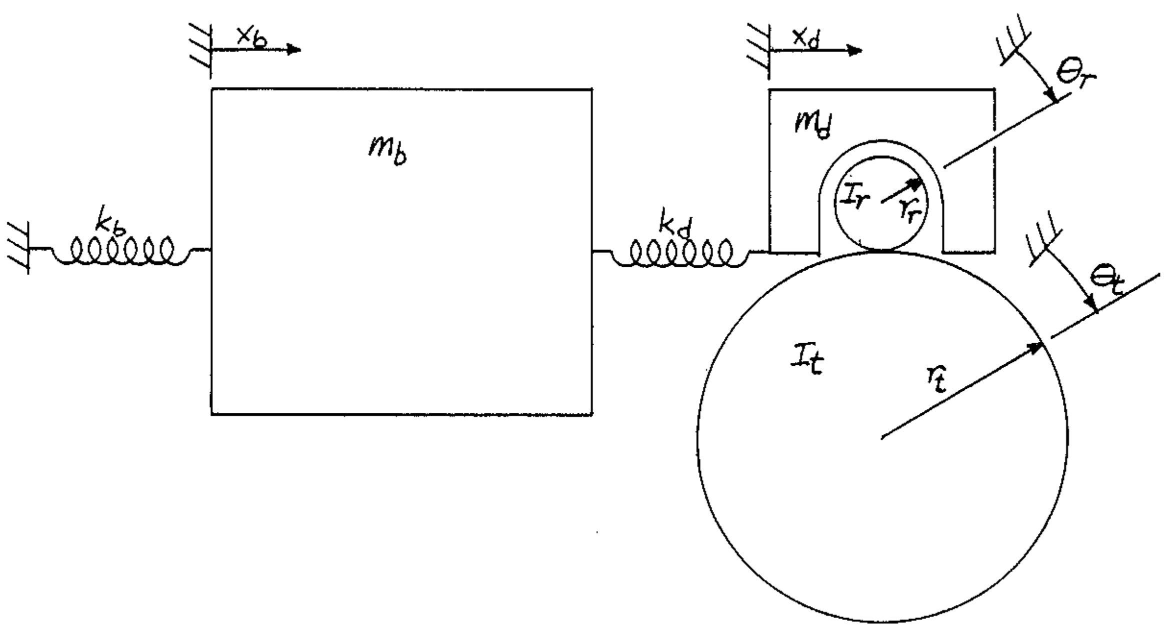


**Figure 1:** Simplified model of the azimuth axis of a telescope. The meanings of the symbols are given in Appendix A.

The model parameters we use could represent a large telescope and in particular could apply to the Magellan Project 8-m. The parameters are listed in Table 1.

Table 1

| | | | |
|---|---|---|---|
| $I_t$ | Telescope inertia | $5x10^6$ | $kg*m^2$ |
| $I_r$ | Drive line (rotor) inertia | 1 | $kg*m^2$ |
| $m_d$ | Drive box mass | 1000 | kg |
| $m_b$ | Base (pier) mass | $10^6$ | kg |
| N | Drive ratio | 40 | |
| $r_t$ | Driven surface radius | 4 | m |
| $f_b$ | Base (pier) resonant frequency | 10 | Hz |
| $f_d$ | Drive resonant frequency | 50 | Hz |

The pier resonant frequency, $f_b$, is calculated using the pier mass on the compliance, $k_b$. The drive resonant frequency, $f_d$, is calculated using both the drive mass and rotor inertia on the drive compliance, $k_d$. The result of this is that the individual resonant frequencies appear very distinctly in the overall frequency response and are therefore easy to identify. Also, since these modes are nearly independent of the rest of the system, they are relatively easy to use as design criteria and to measure on a real structure.

Note that the output side of the drive box is considered to be rigid compared to the other compliances. This seems to be a reasonable assumption, especially for a single stage friction drive where the output shaft can be a stiff element.

Throughout this analysis, we use torque at the drive rotor as the input to the system. The output of the system is the telescope's position relative either to the pier or to inertial space, depending on the case under consideration. Most telescopes presently use measurements relative to the pier for position encoding, but inertial measurements do appear to have some advantages, as we will show.

## DESCRIPTION OF THE RESULTS

The magnitude and phase response for the model system are illustrated in Figure 2. The important features shown in figure 2a are the resonance with a preceding antiresonance near 10 Hz, and the resonance with a following antiresonance near 50 Hz. The phase response in Figure 2b shows an area of phase lead associated with the resonance near 10 Hz, and an area of phase lag associated with the resonance near 50 Hz. The area of phase lag is particularly detrimental in that it sets a practical limit on the servo crossover frequency. The area of phase lead is not as damaging, but disturbance rejection will be degraded because of it.

To give a feel for the sensitivity of the system, we varied several parameters one at a time and calculated the results. Figure 3a shows the magnitude response of the system when the drive ratio, N, is changed from 40 to 400. The major features are the same as in the

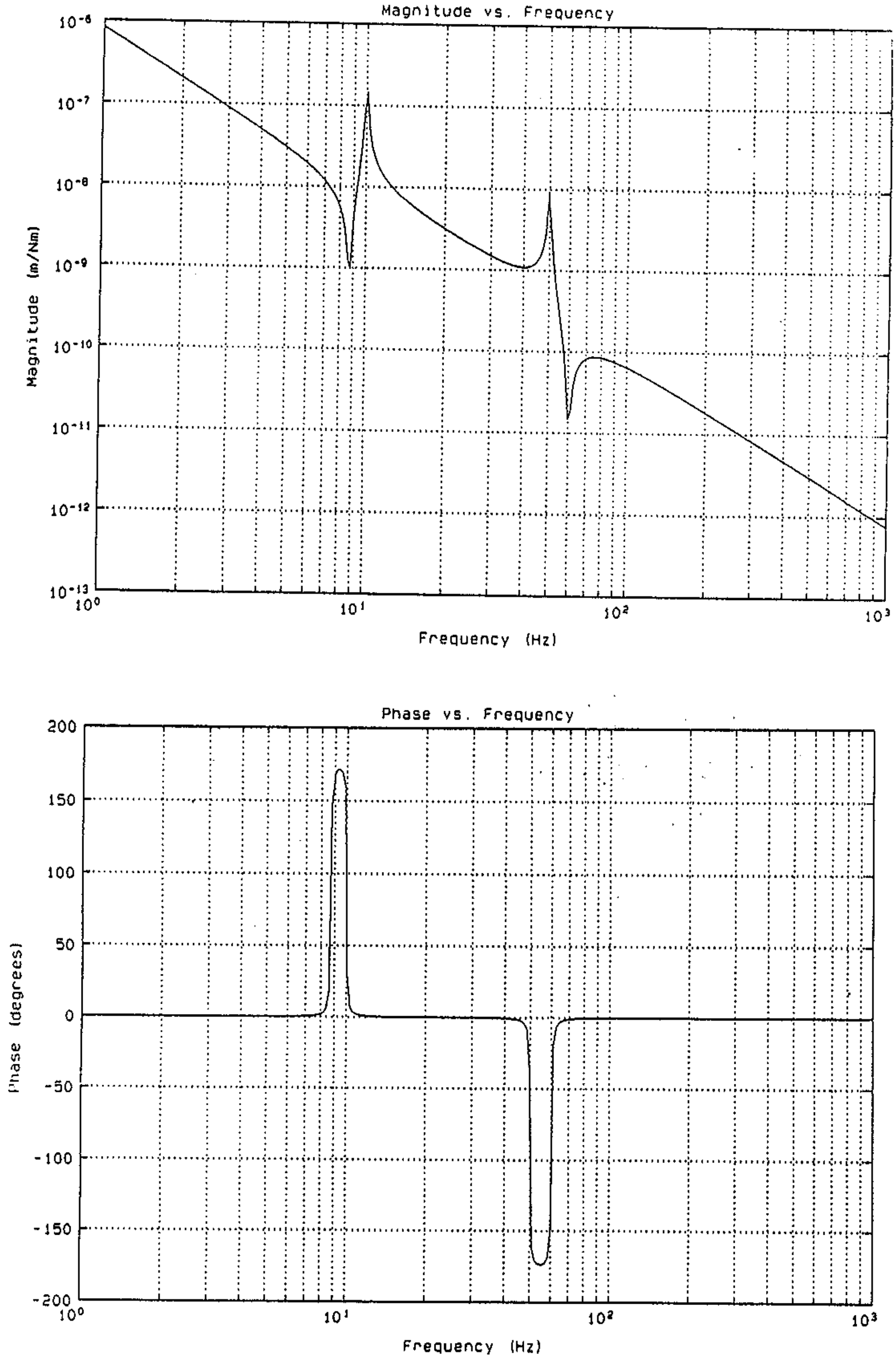


**Figure 2a,b:** Magnitude and phase responses for the model system.

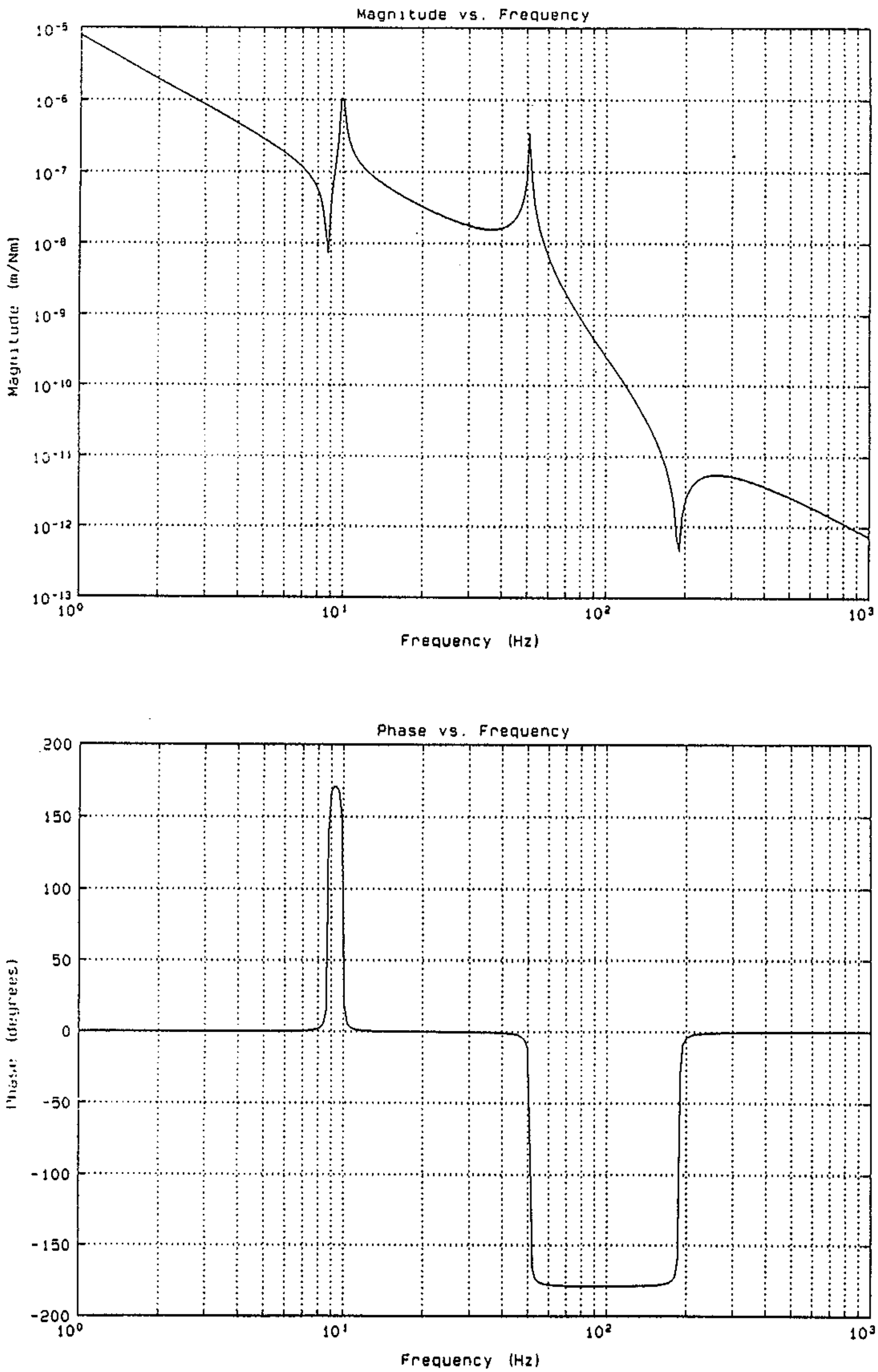


**Figure 3a,b:** Magnitude and phase responses for the model system with the drive ratio, N, raised from 40 to 400.

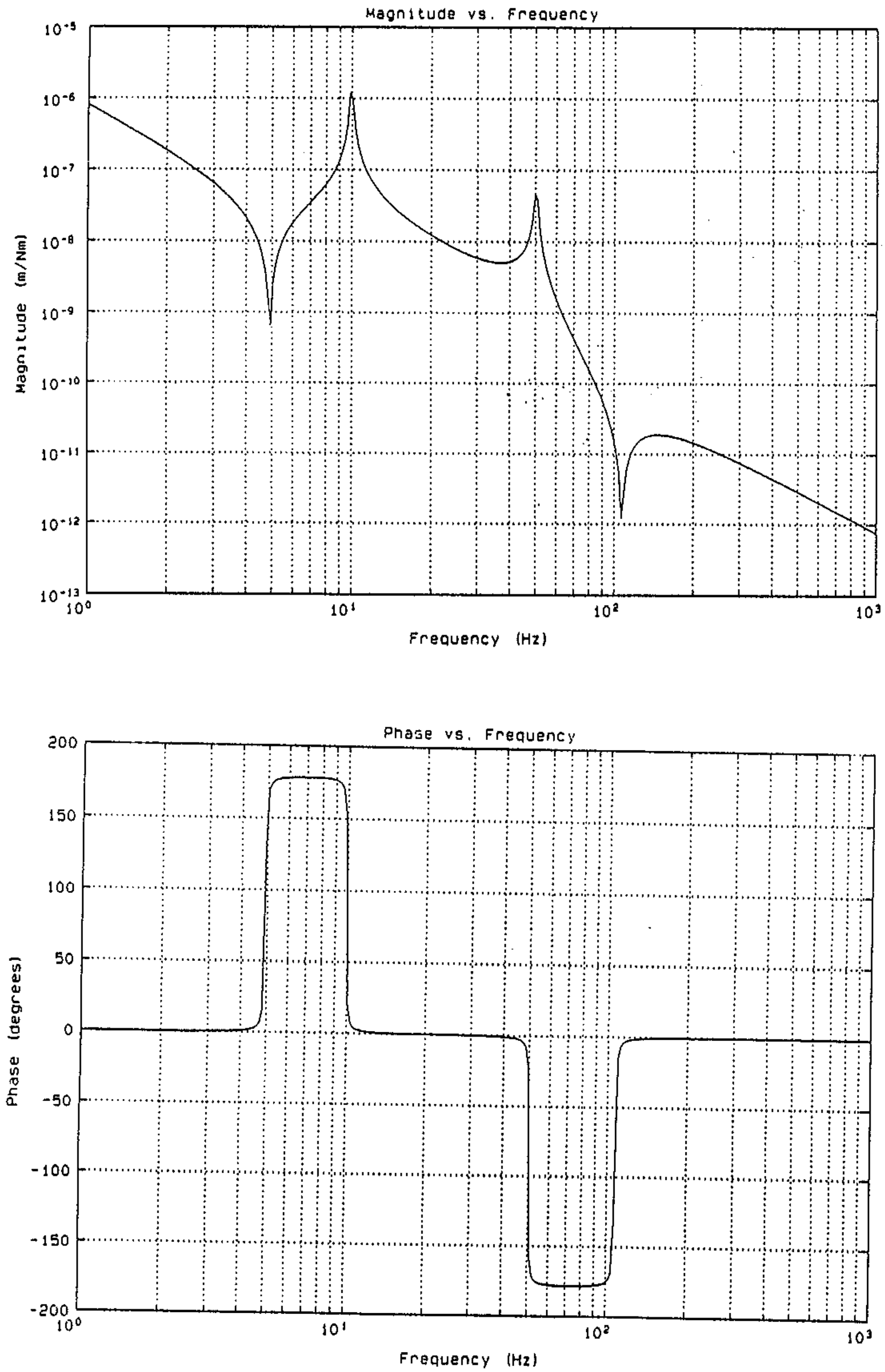


**Figure 4a,b:** Magnitude and phase responses for the model system with the pier mass, $m_b$, lowered from $10^6$ kg to $10^5$ kg.

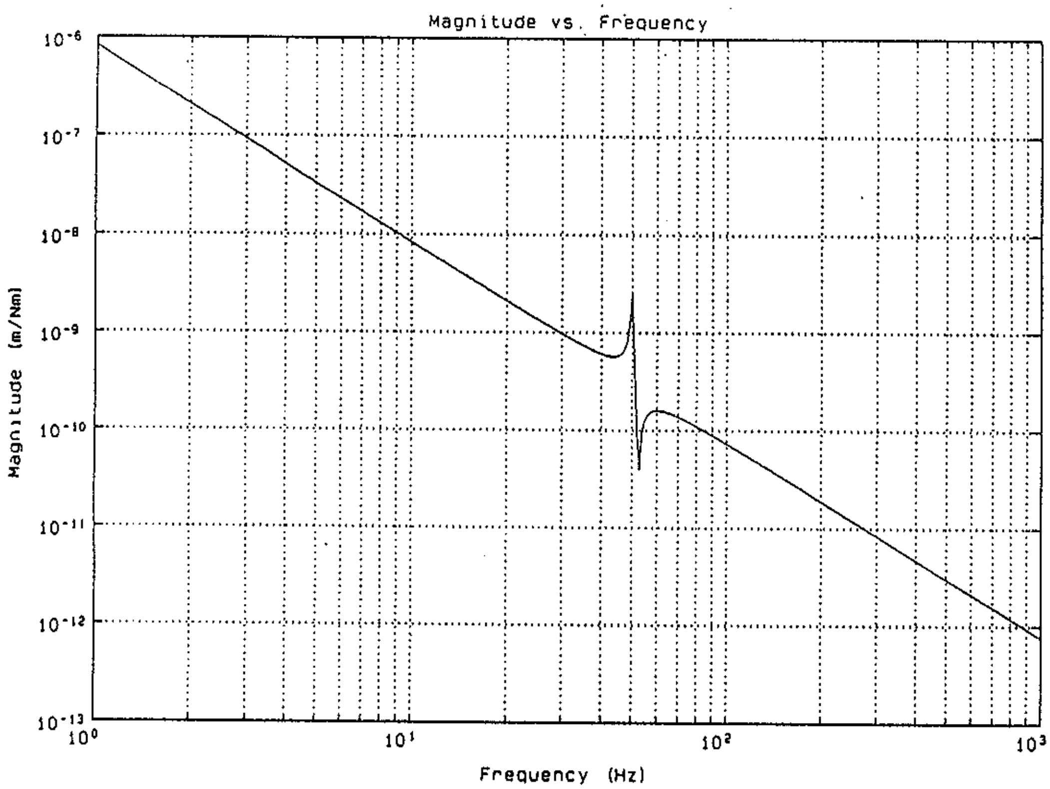


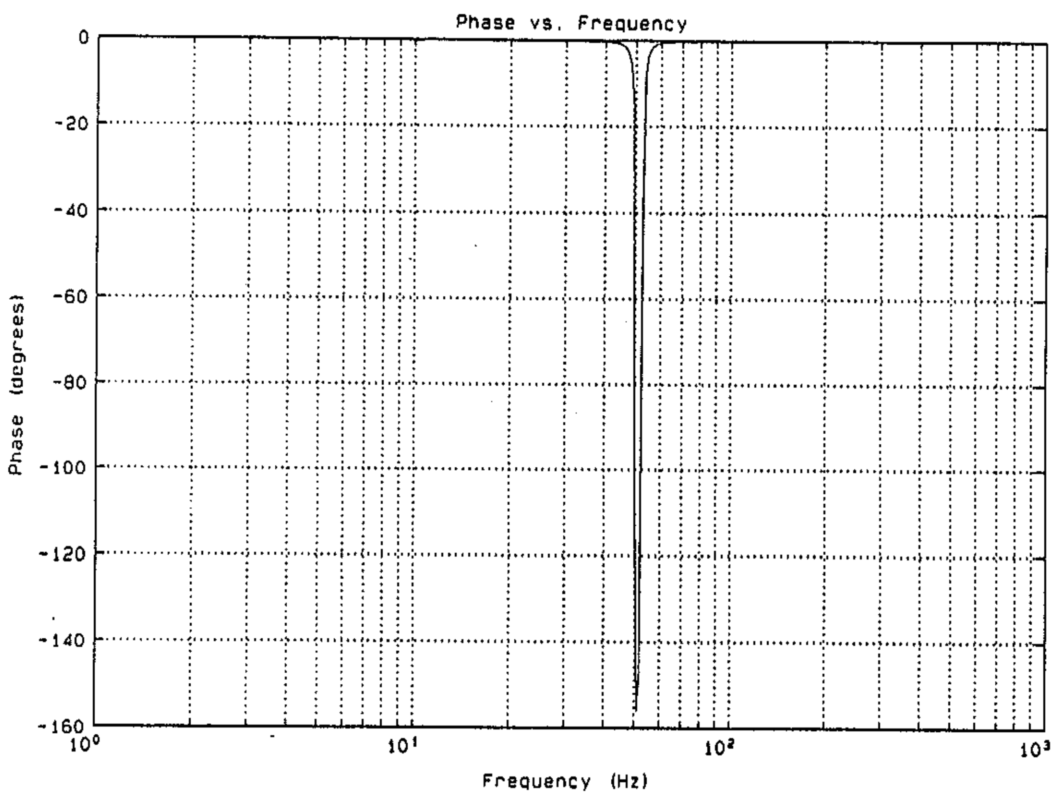


**Figure 5a,b:** Magnitude and phase responses for the model system using inertial encoding of the axis position.

case shown in Figure 2; that is, in Figure 3a there are still two antiresonance-resonance pairs with the resonances near 10 Hz and 50 Hz. The obvious change is that the high frequency antiresonance has moved to an even higher frequency. This results in the widening of the area of phase lag as shown in Figure 3b. A more subtle change has also occurred in that the height of the 50 Hz resonance peak relative to the low frequency behavior has increased by about a factor of 3. This would have the practical result of a lower servo crossover frequency.

Figure 4 shows the magnitude and phase response for the system when the mass of the pier has been decreased from $10^6$ kg to $10^5$ kg. Again, the major features of the magnitude response are the same with two antiresonance-resonance pairs. This time however, both antiresonances have moved toward the extremes--the low frequency antiresonance to a lower frequency, and the high frequency resonance to a higher frequency. Relative to the low frequency behavior, the height of the 50 Hz peak has again increased, this time by a factor of about 5. As before, this increase in the height of the resonance peak will result in a lower crossover frequency. A further and perhaps more significant effect in this case is the deepening and widening of the antiresonance below 10 Hz. This will very strongly degrade the disturbance rejection of the system in the area in and around 3 Hz to 9 Hz.

Figure 5 depicts the magnitude and phase response for the model system when the position of the telescope is measured relative to inertial space. The results in this case are qualitatively different from the previous cases. Now only the high frequency antiresonance-resonance pair is evident, and the peak-to-valley amplitude is about 15 times smaller that in Figure 2. This system would have better disturbance rejection and a higher servo crossover frequency, resulting in markedly better performance overall. For completeness it should be noted that these advantages of inertial measurements decrease as the pier mass decreases, but the effect in this system is rather weak. It requires a reduction by a factor of 10 in the pier mass for the degradation to become at all noticeable in this instance.

## IMPLICATION OF THE RESULTS

The results illustrated in Figure 2 are a reasonable representation of what we might see in a real telescope design. These results indicate that the flexibility due to the pier will primarily degrade disturbance rejection, and the flexibility in the drive box support will primarily limit the servo crossover frequency. Of the two, the flexibility in the drive support is probably the most important in the performance of the final system.

The detrimental effects of pier flexibility would be more serious under the rather extreme condition that the pier were very small with little mass. This is the case illustrated in Figure 4 where the pier mass has been reduced by a factor of 10. The result is poor servo bandwidth and poor disturbance rejection. Fortunately, this probably does not represent any sort of reasonable ground based telescope.

When the drive ratio is increased as illustrated in Figure 3, the primary effect is a lowering of the servo crossover frequency and a corresponding degradation of the system performance. The case illustrated is perhaps a bit misleading since raising the drive ratio would most likely be accompanied by a reduction of the drive rotational inertia (a smaller motor, if nothing else), with the smaller inertia tending to cancel the ill effects of the higher ratio. Nevertheless, the overall advantage in this regard still seems to lie with the lower drive ratios since complete cancellation requires that the inertia vary as the inverse square of the drive ratio. This may not be feasible in all cases.

The results obtained by assuming the use of inertial position measurement and illustrated in Figure 5 indicate that a noticeable performance improvement is possible. The most straightforward system would support a conventional encoder on a structure which is in turn supported directly by the ground. This structure bypasses the "flexible" pier. The encoder structure would clearly have some flexibility, but it would be much less critical than the pier flexibility since it is not loaded by the drive forces and is not in the feedback path. The encoder structure would need to resist only the disturbance forces that are present.

Alternatively, for inertial measurements gyros or accelerometers directly on the telescope axis could be used. In the frequency the range above 0.1 Hz, the performance of these devices can be excellent, with even mechanical gyros obtaining unmodelled drifts of 0.001 arcseconds per second RMS. The inherent low frequency errors of these devices can be removed with a conventional position encoder.

## CONCLUSIONS

Overall, stiff and massive piers are desirable for the sake of disturbance rejection, with stiffness more important than mass for a normal telescope. That is to say, mass in the pier is desirable so long as the resonant frequency remains high. For the analysis of this report, the pier mass and frequency seem to be in good engineering proportion with the rest of the system.

The resonant frequency of the drivebox on its support should also be high since this represents a mode that can limit the servo crossover frequency. 50 Hz as used in this analysis could be considered the minimum acceptable, and 100 Hz is not excessive. This is especially true when the additional phase lag of the other limiting modes (not addressed here) is included.

As frosting on the cake, or as a solution to a difficult problem, using inertial references for axis position measurement can result in improved performance. This is particularly true if the pier flexibility is otherwise very noticeable in the system behavior.

# APPENDIX A

System Dynamics

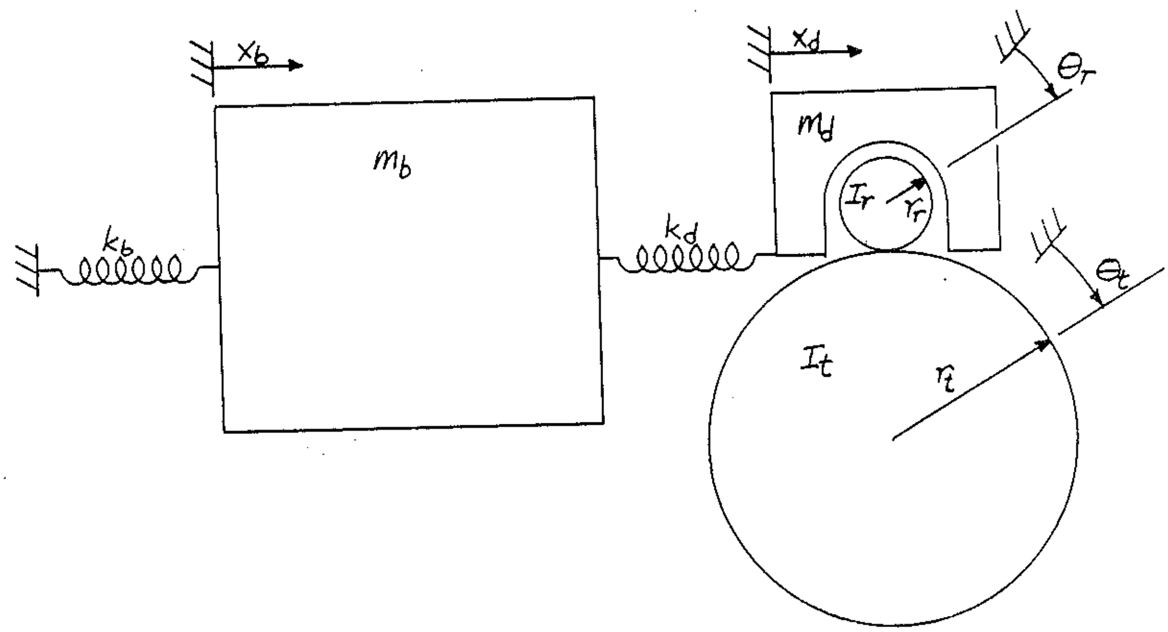


Refering to the figure above, we use the Lagrangian formalism to derive the equations of motion. The symbols used in this derivation are:

- $I_t$ = "Telescope" inertia.
- $I_r$ = "Rotor" (drive line) inertia.
- $m_d$ = Drive box mass.
- $m_b$ = Base (pier) mass.
- $k_d$ = Drive compliance.
- $k_b$ = Base compliance.
- $\theta_t$ = Inertial telescope angle.
- $\theta_r$ = Inertial rotor angle.
- $x_d$ = Inertial drive position.
- $x_b$ = Inertial base position.
- $r_t$ = Radius of driven surface.
- $r_r$ = Radius of driving surface.
- $\tau_r$ = Torque applied at the rotor.

We selected as the generalized displacements

$q_1 = \theta_t$,
$q_2 = \theta_r$,
$q_3 = x_b$,

with the auxiliary equation

$$x_D = (r_t - r_r)\left(\theta_t + \theta_r \frac{r_r}{r_t}\right),$$

Considering now the kinetic energies, we find

$$T_t = \frac{1}{2} I_t \dot{\theta}_t^2,$$

$$T_r = \frac{1}{2} I_r \dot{\theta}_r^2,$$

$$T_d = \frac{1}{2} m_d \dot{x}_d^2,$$

$$T_b = \frac{1}{2} m_b \dot{x}_b^2,$$

so that the total kinetic energy is, in terms of the generalized displacements,

$$T = \frac{1}{2}\left[\dot{q}_1^2 (I_t + (r_t - r_r)^2 m_d) + \dot{q}_2^2 \left(I_r + \left(\frac{r_r}{r_t}\right)^2 (r_t - r_r)^2 m_d\right) + \dot{q}_3^2 m_b + 2\dot{q}_1 \dot{q}_2 \frac{r_r}{r_t}(r_t - r_r) m_d\right].$$

For the generalized forces corresponding to the generalized displacements we find

$$Q_1 = -\tau_r + k_d\left(q_3 - (r_t - r_r) q_1 - \frac{r_r}{r_t}(r_t - r_r) q_2\right)(r_t - r_r)$$

$$Q_2 = \tau_r + k_d\left(q_3 - (r_t - r_r) q_1 - \frac{r_r}{r_t}(r_t - r_r) q_2\right)\frac{r_r}{r_t}(r_t - r_r)$$

$$Q_3 = k_d\left((r_t - r_r) q_1 + \frac{r_r}{r_t}(r_t - r_r) q_2\right) - (k_b + k_d) q_3$$

Since this system is externally forced by $\tau_r$, we apply Lagrange's equation for nonconservative systems,

$$\frac{d}{dt}\left(\frac{\partial T}{\partial \dot{q}_i}\right)-\frac{\partial t}{\partial q_i}=Q_i$$

for i = 1,2,3.
Letting

$$a=(r_t-r_r),$$

$$c=\frac{r_r}{r_t}(r_t-r_r),$$

yields the equations of motion

$$\ddot{\theta}_t(I_t+a^2m_d)+\ddot{\theta}_r acm_d=-\tau_r+k_d(x_b-a\theta_t-c\theta_r)\,a$$

$$\ddot{\theta}_r(I_r+c^2m_d)+\ddot{\theta}_t acm_d=\tau_r+k_d(x_b-a\theta_t-c\theta_r)\,c$$

$$m_b\ddot{x}_b=k_d(a\theta_t+c\theta_r)-x_b(k_b+k_d)$$

For numerical calculations, these equations are rearranged into the state-space form

$AX + BU = \dot{X}$

$CX + DU = Y$

with the following meanings for the symbols.

$$X = [\theta_t \;\; \dot{\theta}_t \;\; \theta_r \;\; \dot{\theta}_r \;\; X_b \;\; \dot{X}_b],$$

$U = \tau_r$,

Y = system output,

$$B = [0 \;\; a_8 \;\; 0 \;\; a_4 \;\; 0 \;\; 0],$$

$$c = [-r_t \; 0 \; 0 \; 0 \; 1 \; 0],$$

$$D = 0$$

$$A = \begin{bmatrix} 0 & 1 & 0 & 0 & 0 & 0 \\ a_5 & 0 & a_6 & 0 & a_7 & 0 \\ 0 & 0 & 0 & 1 & 0 & 0 \\ a_1 & 0 & a_2 & 0 & a_3 & 0 \\ 0 & 0 & 0 & 0 & 0 & 1 \\ k/m_b & 0 & l/m_b & 0 & -m/m_b & 0 \end{bmatrix},$$

$$a = r_t - r_r,$$

$$b = \frac{r_r}{r_t},$$

$$d = (I_r I_t) + m_d a^2 (I_r + b^2 I_t),$$

$$k = a k_d,$$

$$l = a b k_d,$$

$$m = k_d + k_b,$$

$$a_1 = -I_t a^2 b k_d / d,$$

$$a_2 = -I_t a^2 b^2 k_d / d,$$

$$a_3 = I_t a b k_d / d,$$

$$a_4 = (I_t + a^2 m_d (1+b)) / d,$$

$$a_5 = -I_r a^2 k_d / d,$$

$$a_6 = -I_r a^2 b k_d / d,$$

$$a_7 = I_r a k d / d,$$

$$a_8 = -(I_r + a^2 m_d (b^2 + b)) / d.$$

# APPENDIX B

## Plot Generating Program

```
% springb5.m
% This file runs in Matlab.
% Calculates the frequency response of a three body system where the
% load is rigid and the driving member is connected by a compliance
% to a mass that itself is connected by a compliance to ground.
% The model takes the roatational inertia of the drive motor and
% capstan explicitly into account. A single stage of reduction is assumed.
% (i.e., the capstan to the axis).  The
% input is a torque between the drive box and motor rotor, and the output
% is the position of the load relative to the mass adjacent to ground.
% This simulates driving a telescope off of a springy pier or altitude
% support, and encoding the position of the axis relative to that support.
%
% Caution:  The routine "ss2zp" is numerically unstable and will give
% wrong answers for some parameter values.  Always check your results
% against results obtained by using the A, B, C, and D matrices directly.
% This can be done by commenting out the line containing the call to the
% routine "zp2ss".

It=5e6;  %Inertia of the "telescope".
mb=1e6;  %Mass of the base or "pier".
md=1000;    %Mass of the "drive box" and motor.
Ir=1;   %Inertia of drive motor and capstan.
fd=50;  %Frequency of the drive box alone on its support.
rt=4;  %Radius of telescope drive surface.
N=40;  %Drive ratio.
rr=rt/N; %Drive roller radius.
kd=(2*pi*fd)^2*(md+(Ir/rr^2));  %"Drive box" (tangent arm) stiffness.
                                %Accounts for rotor inertia.
fb=10;   %Frequency pier on pier stiffness.
kb=(2*pi*fb)^2*(mb); %"Pier" stiffness.


a=rt-rr;
b=rr/rt;

k=a*kd;
l=a*b*kd;
m=kd+kb;

d=Ir*It + md*a^2*(Ir + b^2*It);

a1=-It*a^2*b*kd/d;
a2=-It*a^2*b^2*kd/d;
a3=It*a*b*kd/d;
a4=(It + a^2*md*(1+b))/d;
a5=-Ir*a^2*kd/d;
a6=-Ir*a^2*b*kd/d;
a7=Ir*a*kd/d;
a8=-(Ir + a^2*md*(b^2+b))/d;


A=[     0       1       0       0       0       0

        a5      0       a6      0       a7      0

        0       0       0       1       0       0

        a1      0       a2      0       a3      0
```

```
        0         0         0         0         0         1
        k/mb      0         1/mb      0         -m/mb     0];
B=[     0
        a8
        0
        a4
        0
        0];
C=[-rt       0         0         0         1         0];
D=0;
fs=logspace(0,3,400);

% This next bit adds a small amount of damping to make the plots more
% realistic.  Unfortunately, "ss2tf" uses an unstable algorithm (there is
% no other) and will result in obviously wrong answers for some parameter
% values. To be safe, check your results against those obtained when the
% line containing the call to "zp2ss" is commented out.

[num,den]=ss2tf(A,B,C,D,1);
zeros=roots(num);
poles=roots(den);
zeros=zeros-0.005*sqrt(zeros .* conj(zeros)); %Add damping.
poles=poles-0.005*sqrt(poles .* conj(poles));
zstrt=length(num)-length(poly(zeros))+1;
k=abs(num(zstrt:length(num))/poly(zeros));
[A,B,C,D]=zp2ss(zeros,poles,k);

[mag,phase]=bode(A,B,C,D,1,2*pi*fs);

loglog(fs,mag),grid %Generate the plots.
title('Magnitude vs. Frequency')
xlabel('Frequency (Hz)')
ylabel('Magnitude (m/Nm)')
pause

YN=input('Save the plot? Y/N [N]:','s');
if isempty(YN)
        YN='N';
end

if YN~='N'
        meta d:\matlab\wiyn\spring5plot
end

semilogx(fs,phase+180),grid
title('Phase vs. Frequency')
xlabel('Frequency (Hz)')
ylabel('Phase (degrees)')
pause


YN=input('Save the plot? Y/N [N]:','s');
if isempty(YN)
        YN='N';
end

if YN~='N'
        meta d:\matlab\wiyn\spring5plot
end
```